Effect of gravity on stable Saffman-Taylor fingers

Efim Brener,* Marc Rabaud, and Henry Thomé
Laboratoire de Physique Statistique de L'Ecole Normale Supérieure, 24 rue Lhomond, 75231 Paris Cedex 05, France
(Received 26 March 1993)

A theoretical and experimental study of transverse gravity effects is presented for stable Saffman-Taylor fingers propagating in a linear tilted cell. In the high-velocity limit, the experimental results are compared to the theoretical work of Brener, Levine, and Tu [Phys. Fluids A **3**, 529 (1991)]. As predicted, when the tilt angle is increased, the finger becomes narrower and more asymmetrical as it becomes located nearer to the upper lateral boundary. In the limit of low velocities, a theory for the gravity effect is presented and its predictions are experimentally checked.

PACS number(s): 47.20.Hw, 47.15.Hg, 47.60.+i, 68.10.−m

I. INTRODUCTION

In the last decade, a large amount of work has been devoted to the understanding of the Saffman-Taylor instability as a simple example of pattern-forming systems [1]. In their pioneering work, Saffman and Taylor [2] demonstrated that curved interfaces can propagate steadily in a long and narrow Hele-Shaw cell when a viscous fluid is displaced by a less viscous one. For very small velocities such a Saffman-Taylor (ST) finger fills the whole cell. For increasing velocities, it becomes narrower and finally occupies half of the width of the channel. Neglecting surface tension, these authors found by conformal transformation an analytic solution for any relative width λ. The question of the selection of the width by surface tension was solved only recently [3] and precise measures of the selected λ can be found in Tabeling, Zocchi, and Libchaber [4]. Since then, it has been shown that the asymptotic value $\lambda = 0.5$ can be broken by introducing localized anisotropy in the cell [5] or singular perturbation of the fingers tip [6].

These analytical zero surface tension solutions for the shape of the meniscus have been extended to various other conditions. Ben Amar and simultaneously Yuhai Tu [7] found solutions for divergent Hele-Shaw cells, following the experimental and analytical work of Thomé *et al.* [8], who demonstrated the existence of self-similar growth in divergent channels. Rabaud and Hakim [9] showed the possibility to obtain analytical shapes for fingers propagating in a direction making an angle with the flow axes, a case related to traveling interface in directional viscous fingering [10] or in directional-solidification experiments [11]. Taylor and Saffman [12] have shown that noncentered fingers are also solutions of the basic equations without surface tension. Until now these asymmetrical fingers had been only observed using localized perturbations (for example, stretching along the cell a thin off centered wire) [13,14]. The stability of such perturbed fingers was analyzed by Hong [15], and it was demonstrated [16,17] that asymmetrical fingers are not naturally selected. However, it is only recently that Brener, Levine, and Tu [18] showed that this would be the case if the gravity field acts on a Hele-Shaw cell tilted around the flow axis. These authors found the fingers shape at zero surface tension, investigated the selection theory and gave power-law predictions in the limit of small-capillary and gravity effects. In the present paper, as suggested in Ref. 15, the effect of gravity is experimentally investigated for stable ST fingers propagating in these linear cells [19]. We also extend the theory as well as the experiment into the limit of low velocity, where the fingers fill a large portion of the channel.

The outline of the present paper is as follows. In the next section the theory of nonsymmetric ST fingers in the low-velocity limit is presented. Afterwards we present the experimental setup and the experimental results for large as well as for low propagating velocity. Finally, a discussion forms the last section.

II. THEORETICAL SELECTION OF LARGE FINGERS

In the present section we consider theoretically the problem of a nonsymmetric ST finger in the limit where the finger moves at low velocity and fills the channel almost completely. In this limit, where surface-tension effects play a dominant role and cannot be treated as a perturbation, the theory of the symmetric ST finger has been developed by Dombre and Hakim [20]. Their treatment is analogous to the analysis of coating films done by Landau and Levich [21]. The idea is that the tip region (outer region) and the trailing part (inner region) of the finger can be treated separately and can be matched afterwards. In the presence of a nonsymmetric gravitational force, the inner equation and the matching conditions remain unchanged because of the small scale, and the outer equation containing asymmetry can be solved exactly. We find that for a given tilt angle the finger sticks at the top sidewall for some critical minimal velocity (as for a symmetric finger) but does not fill the whole channel. This critical velocity decreases and the finger width decreases if the rotational angle increases.

Let us recall the basic formulation of the ST problem in the presence of a nonsymmetric gravitational force.

1063-651X/93/48(2)/1066(7)/$06.00

A viscous fluid obeying Darcy's law $\mathbf{v} = -(q/\mu)\nabla p$ is displaced by a second fluid of negligible viscosity. Here $\mathbf{v}$ is the two-dimensional velocity, p is the pressure field, μ the viscosity, $q = b^2/12$ is the medium permeability, and b is the plate spacing. Assuming incompressibility, the velocity potential $\Phi = -(q/\mu)p$ satisfies Laplace's equation

$$\nabla^2\Phi = 0. \tag{1}$$

For a steady-state finger advancing at a constant velocity V along the x direction the boundary conditions are

$$\frac{\partial\Phi}{\partial n} = V\cos\theta, \tag{2}$$

$$\Phi = (q/\mu)(TK - \rho g y \sin\omega), \tag{3}$$

$$\left(\frac{\partial\Phi}{\partial y}\right)\Big|_{y=\pm W/2} = 0. \tag{4}$$

Here θ is the angle between the local normal vector $\mathbf{n}$ on the interface and the x direction, T is the surface tension, K the local curvature, ρ the fluid density, g the gravitational acceleration, ω the tilt angle, and W is the width of the channel (Fig. 1). We are interested in the limit of low velocity, where the finger fills the channel almost completely. In the tip region the fluid is weakly perturbed by the existence of the thin layers near the sidewalls, the flow is uniform [20]:

$$\Phi = Vx, \tag{5}$$

and the interface profile obeys Eq. (3)

$$BK = x_{\text{int}} + \sigma y_{\text{int}}, \tag{6}$$

where all lengths are divided by the width of the channel W; B and σ are two dimensionless control parameters defined by

$$B = \frac{T}{12\mu V}\left(\frac{b}{W}\right)^2 \tag{7}$$

and

$$\sigma = \rho g \sin\omega\left(\frac{b^2}{12\mu V}\right). \tag{8}$$

Using the following parametrization of the shape:

$$x(\theta) = -\int d\theta \sin\theta/K, \tag{9}$$

$$y(\theta) = \int d\theta \cos\theta/K, \tag{10}$$

and differentiating Eq. (6) with respect to the angle θ, we find

$$BK\left(\frac{dK}{d\theta}\right) = -\sin\theta + \sigma\cos\theta, \tag{11}$$

and finally

$$K = [(2/B)(\cos\theta + \sigma\sin\theta + C)]^{1/2}. \tag{12}$$

This expression for K contains a nonsymmetric term proportional to σ and corresponds to Eq. (9) of Ref. [20] for $\sigma = 0$. The integration constant C can be found by matching solution (12) to the solution in the inner region. Note that C as well as σ should be small since a small curvature and a small contact angle are required for the matching to the inner region. In the narrow gaps between the finger and the sidewalls the potential Φ can be taken as a constant across the thickness of the layer and equal to its value (3) on the interface. This approximation allows us to derive an ordinary differential equation for the shape of the gap. Following directly the derivation of Ref. [20], we get

$$h_i(x)\left(B\frac{d^3h_i}{dx^3} \pm \sigma\frac{dh_i}{dx} - 1\right) = -\delta_i. \tag{13}$$

Here $i = t, b$ and the indexes t and b denote the top and bottom gaps, respectively; $h_i(x)$ is the local thickness of the layer: $h_t(x) = \frac{1}{2} - y_t(x)$ and $h_b(x) = -\frac{1}{2} + y_b(x)$; $\delta_i \ll 1$ is the asymptotic value of the thickness, which is now different for the top and bottom gaps. Using the rescaling $x = (\delta_i B)^{1/3}\tilde{x}$ and $h_i = \delta_i\tilde{h}_i$ we arrive at the parameterless equation

$$\tilde{h}\frac{d^3\tilde{h}}{d\tilde{x}^3} = \tilde{h} - 1, \tag{14}$$

which is identical to the equation given in Ref. [20]. In this rescaled equation we have neglected the term $\sigma\delta_i^{2/3}B^{-1/3}d\tilde{h}/d\tilde{x}$ since $\delta_i \ll 1$.

As shown in Ref. [20] Eq. (14) has the following asymptotic behavior: for $\tilde{x} \to -\infty$

$$\tilde{h} = 1 + \alpha\exp(\tilde{x}) \tag{15}$$

and for $\tilde{x} \to \infty$

$$\tilde{h} = \tilde{x}^3/6 + \beta\tilde{x}^2/2 + \eta\tilde{x} + \tau - 3\ln(\tilde{x}), \tag{16}$$

where α, β, η, and τ depend on the origin of $\tilde{x}$, but the quantity

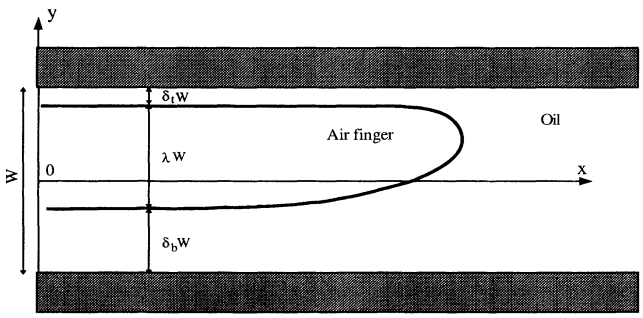

FIG. 1. Sketch of the Hele-Shaw cell with an asymmetrical air finger propagating from left to right at constant velocity.

$$\eta^* \equiv \eta - \beta^2/2 \approx 3.18 \tag{17}$$

is translationally invariant [20]. The matching procedure is very similar to that in Ref. [20], the only difference being that we have two matching conditions for the bottom and top gaps:

$$\theta_{mb} = -\pi/2 + B^{-1/3}\delta_b^{2/3}\eta, \tag{18}$$

$$\theta_{mt} = \pi/2 - B^{-1/3}\delta_t^{2/3}\eta, \tag{19}$$

$$K_{mi} = B^{-4/3}\delta_i^{2/3}\beta^2. \tag{20}$$

The index m denotes the matching point. Combining Eqs. (12) and (17)–(20), we get

$$\delta_b^{2/3} = B^{1/3}(|C| + \sigma)/\eta^*, \tag{21}$$

$$\delta_t^{2/3} = B^{1/3}(|C| - \sigma)/\eta^*. \tag{22}$$

Finally, the condition which allows us to find the integration constant C is that the meniscus fills the channel almost completely. From Eqs. (10) and (12) we get

$$(B/2)^{1/2}\int_{\theta_{mb}}^{\theta_{mt}} \frac{d\theta\cos\theta}{(\cos\theta + \sigma\sin\theta + C)^{1/2}} = 1. \tag{23}$$

We can expect that C and σ will be of the order of $\delta_i^{2/3}$ [see Eqs. (21) and (22)]. It means that in Eq. (23) we can replace the limits of integration by $-\pi/2$ and $\pi/2$ and neglect the nonsymmetric term $\sigma\sin\theta$ at the denominator (by symmetry the integration gives only a quadratic dependence on σ). By this simplification we get the expression for C, which is identical to the expression given in Ref. [20]:

$$C = -A(B^* - B), \tag{24}$$

$$B^* = \frac{1}{2[\int_0^{\pi/2}(\cos\theta)^{1/2}d\theta]^2} \approx 0.348, \tag{25}$$

$$A = \frac{\int_0^{\pi/2}(\cos\theta)^{1/2}d\theta}{B^*\int_0^{\pi/2}(\cos\theta)^{-1/2}d\theta} \approx 1.31. \tag{26}$$

Combining Eqs. (21), (22), and (24), we get the final result for the thickness of the gaps as a function of the control parameters B and σ

$$\delta_b^{2/3} = (B^*)^{1/3}[A(B^* - B) + \sigma]/\eta^*, \tag{27}$$

$$\delta_t^{2/3} = (B^*)^{1/3}[A(B^* - B) - \sigma]/\eta^*. \tag{28}$$

These predictions generalize Eq. (25) of Dombre and Hakim [20]. The numerical value of η^* [Eq. (17)] has been corrected in agreement with Ref. [11] of Ref. [22]. Note that all constants in Eqs. (27) and (28) come from the theory of the symmetrical finger. The dependence on the nonsymmetric parameter σ is remarkably simple. The main effect of gravity is just a rotation of the outer meniscus by a small angle σ [see Eq. (12): $\cos\theta + \sigma\sin\theta \approx \cos(\theta - \sigma)$ for small σ]. In Sec. III C. we will compare our experimental results to these predictions.

III. EXPERIMENTS

A. Experimental setup

Our Hele-Shaw cell is made of two parallel glass plates 15 mm thick, clamped together with Mylar sheet spacers delimiting a cell of length 1300 mm, width $W_1 = 100$ mm, or $W_2 = 17.5$ mm and thickness $b = 0.35$ mm. The narrow channel allows one to obtain large B values with not too small velocity. The inflow and outflow of the fluids occur through two holes drilled in the upper plate. The entire cell can be tilted around the flow axis Ox by an angle ω. This angle is measured with a high-resolution level and wedges assuring a 0.04° resolution. The viscous fluid is a silicon oil, Rhodorsil 47V100, with density $\rho = 965$ kg/m^3 , cinematic viscosity $\nu = \mu/\rho = 10^{-4}$ m^2/s, and surface tension $T = 20.9\ 10^{-3}$N/m at 25°C. The less viscous fluid is air at atmospheric pressure and the interface velocity is adjusted by lowering an oil vessel siphoning the oil out of the cell. The pressure inside the cell is then below atmospheric pressure but flexion of the glass plates can be neglected as we do not use depressions larger than 30 cm of oil. We checked that the finger velocity is almost constant in the central part of the cell. The air-oil meniscus is observed from above, through the upper plate at middle length of the channel by a charge-coupled device (CCD) video camera and digitized with a frame grabber on a Macintosh IIfx computer. All the measures have been done on digitized pictures with one-pixel resolution using the computer program IMAGE.

For each given angle and given level of the oil vessel we measure the velocity V of the propagating finger (resolution ±1%) and the relative widths δ_t and δ_b (resolution ±0.2%) of the remaining oil domains after the finger went by (Fig. 1). From the experimental measures of δ_t and δ_b we calculate the width of the finger by the relation $\lambda = 1 - \delta_t - \delta_b$ and the off-centered parameter $y_0 = (\delta_b - \delta_t)/2$.

In order to compare our results with other works and in particular Ref. [18], we use the dimensionless parameters B and σ defined by Eqs. (7) and (8). The parameter B measures the importance of capillary effects in all linear geometries, by comparing the natural wavelength of the linear stability analysis to the width of the channel [1]. This parameter differs from the parameter γ introduced in Ref. 15, by a factor 4 ($\gamma = 4B$) as we use W instead of $W/2$ to make the parameter dimensionless. For the same reason, our y_0 parameter is smaller by a factor 2 than the asymmetry parameter of Ref. 15. The second parameter, σ, was first introduced in Ref. 15 and it compares the pressure gradient at the interface to the gravity force. Their ratio $\sigma/B = \rho g\sin\omega W^2/T$ is the Bond number.

B. Experimental results at small B

1. Experiments at constant angle

The first sets of experiments are done at constant tilt angle ω, for increasing velocities until the finger finally becomes unstable. In Fig. 2 we present the evolution of λ and y_0 vs B for various tilt angles.

For horizontal cells ($\omega = 0$), symmetric Saffman-Taylor fingers have a width that increases slowly with B. Due to three-dimensional effects neglected in the usual theory, the existence of a coating film on the glass plates makes the value of λ for small B slightly smaller than 0.5 [4,23]. But, even for small tilt angles ($\omega \geq 2.2°$) we observe fingers with widths decreasing with B. At the same time the asymmetry measured by y_0 becomes large. As shown in Fig. 2, the stability of the fingers at small B increases with the tilt angle. For horizontal cells, stable fingers are not observed for $B < 3 \times 10^{-4}$, while for vertical cells, stable fingers were observed until $B < 5 \times 10^{-5}$. A similar enhancement of the stability has already been observed for narrow fingers [8]. At constant B the decrease of the tip radius by the gravity increases the stability.

In this set of experiments, working at constant angle and changing the velocity, B and σ evolve simultaneously, their ratio being constant.

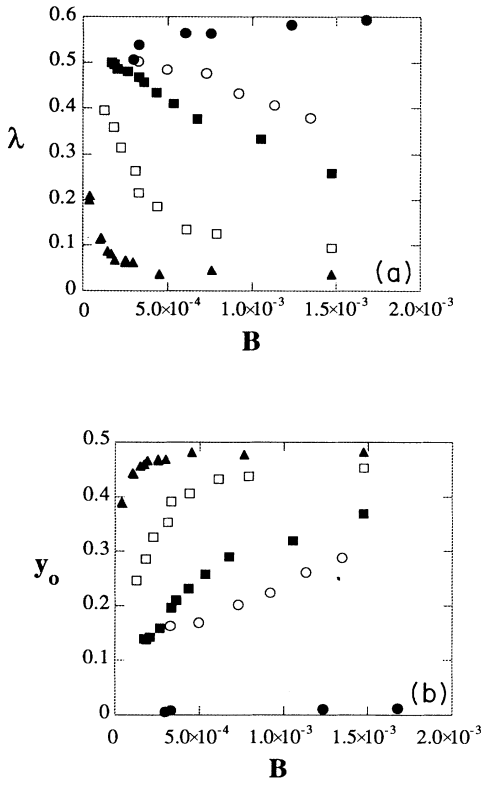

FIG. 2. Evolution of the width λ (a) and y_0 (b) vs B for different tilt angles: $\omega = 0°$ (•), $\omega = 2.2°$ (○), $\omega = 5.06°$ (■), $\omega = 10°$ (□) and $\omega = 90°$ (▲).

2. Experiments at constant B

In order to compare our results to the predictions of Brener, Levine, and Tu [18], where B and σ are supposed to be small and independent parameters, we manage to vary σ (changing ω) at constant B (almost constant velocity). The evolution of λ and y_0 vs σ is presented in Fig. 3 for $B = (0.32 \pm 0.02) \times 10^{-3}$. For large σ, the finger is extremely thin and touches the upper boundary ($\lambda \to 0$ and $y_0 \to 1/2$). It is worth noting that when the tilt angle is large, after the finger has passed by, the upper side of the interface becomes progressively wavy following a Rayleigh-Taylor instability. This deformation evolves to form falling oil drops and filaments [24] that may temporally close to the finger.

3. Comparison with theory

Brener, Levine, and Tu [18] developed a selection theory in the limit of small σ and small B, introducing the parameter ϵ. This parameter is related to σ by

$$\epsilon \approx 2\sigma\lambda/\pi \tag{29}$$

for small σ. These authors derived analytical predictions in three cases depending on the respective values of $\gamma(= 4B)$ and ϵ.

(i) First case, $\epsilon^{3/2} \ll \gamma \ll 1$, the scaling for λ is the same as for symmetrical fingers $(\lambda - 1/2) \sim \gamma^{2/3}$, and for y_0 they found $y_0 \sim \epsilon$.

(ii) Second case, $\epsilon^{5/2} \ll \gamma \ll \epsilon^{3/2}$. They found the scaling $(1/2 - \lambda) \sim y_0^2 \sim \epsilon^{5/2}/\gamma$.

(iii) Third case, $\gamma \ll \epsilon^{5/2}$. They predict the scaling $\lambda \sim (1/2 - y_0) \sim \gamma^{1/3}\epsilon^{-5/6}$.

In our experiment, the parameters are B and σ and we work either at constant tilt angle (B/σ = const), or at constant B changing the σ value. What are the predictions in such cases?

(i) In the first case, i.e., for very small angles and large velocities, the selection of the finger width is unchanged with respect to horizontal cells $(\lambda - 1/2) \sim B^{2/3}$. But a small shift y_0 exists, and increases linearly with σ.

(ii) In the second case, the scaling becomes $(1/2 - \lambda) \sim y_0^2 \sim \sigma^{5/2}/B$. This means that working at constant

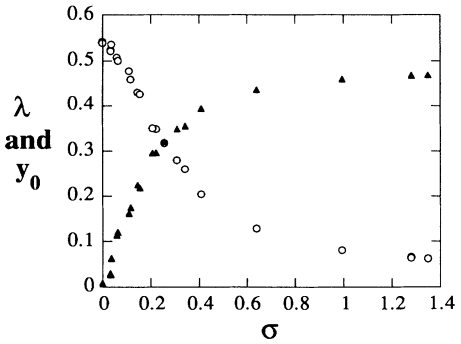

FIG. 3. Evolution of the width λ (○) and y_0 (▲) vs σ for almost constant $B \approx (0.32 \pm 0.02) \times 10^{-3}$.

angle, λ is a decreasing function of B and y_0 an increasing function of B: $(1/2-\lambda) \sim B^{3/2}$ and $y_0 \sim B^{3/4}$. At constant B the scaling is $(1/2-\lambda) \sim y_0^2 \sim \sigma^{5/2}$.

(iii) In the third case, as $\epsilon \sim \sigma\lambda$, the scaling becomes $\lambda \sim (1/2-y_0) \sim B^{2/11}\sigma^{-5/11}$. Then λ is small and y_0 large. For constant B/σ ratio, λ is a decreasing function of B and y_0 an increasing one as $\lambda \sim (1/2-y_0) \sim B^{-3/11}$. At constant B the scaling is $\lambda \sim (1/2-y_0) \sim \sigma^{-5/11}$.

The location of our experimental data in the plane of the two parameters γ and ϵ can be compared with the two limiting curves $\gamma = \epsilon^{3/2}$ and $\gamma = \epsilon^{5/2}$. With the hypothesis of all prefactors equal to one in the scalings, all these points scatter around the line $\gamma = \epsilon^{5/2}$ and the related experiments are then in the crossover between cases (ii) and (iii). The experimental decrease of λ for increasing B at constant B/σ [Fig. 2(a)] or increasing σ at constant B (Fig. 3) is in complete qualitative agreement with the predictions of these two cases, as it is for the increase of y_0 [Figs. 2(b) and 3]. However, the power-law behaviors are only in rough quantitative agreement. This can be ascribed to the fact that the exact asymptotic value is not 1/2 because of three dimensionality [20] and also because experimental fingers are always unstable in the limit of vanishing B. The same reasons explain that the scaling $(\lambda-1/2) \sim B^{2/3}$ of the symmetrical ST fingers was never, to our knowledge, precisely verified experimentally.

4. Shape of nonsymmetrical fingers

Brener, Levine, and Tu [18] solved the ST problem with gravity for zero surface tension. They obtained the analytical shapes of the interface as a triple continuum family of solutions with parameters λ, y_0, and ϵ. Their shapes are given by

$$x = (W/\pi)[(1-\lambda)\ln(\sin 2\alpha) + 2y_0 \ln(\tan\alpha)] \qquad (30)$$

and

$$y = W\left[y_0 - \frac{\lambda}{2} + \frac{2\lambda\cos(\epsilon\pi/2)}{\pi}\int_0^{\alpha}(\tan\alpha')^{\epsilon}d\alpha'\right], \qquad (31)$$

where α runs from 0 to $\pi/2$. This family reduces to the asymmetrical family of Taylor and Saffman [12] for $\epsilon = 0$. For a given experimental finger, we determine the values of the three parameters λ, y_0, and ϵ. It is then easy to compare the real shape to the predicted one. The shapes differ for large B, which is not surprising as the surface tension corrections are then important. But at zero angle and small B (classical narrow ST fingers) the agreement between experimental shapes and analytical ones is very good. Figure 4 compares for $\omega = 5°$ and $B = 0.33 \times 10^{-3}$ the experimental and analytical shapes given by Eqs. (30) and (31). The two shapes are clearly different and this is always the case. It appears that off-centered fingers are theoretically quite asymmetrical at the tip, an asymmetry even enforced by the gravity parameter ϵ. In the experiments, this tip asymmetry seems to be smoothed by surface tension, even if B is small. The agreement would surely be better with numerical resolution of the equations taking surface tension into account, but simple existing computer codes do not include asymmetry of the interface [25].

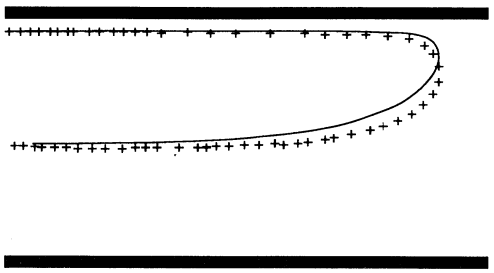

FIG. 4. Shape of an asymmetrical finger for $\epsilon = 0.057$, $\delta_t = 0.07$, and $\delta_b = 0.462$. The points (+) come from the experimental profile; the continuous line is the corresponding analytical solution of Eqs. (30) and (31).

C. Experimental results at large B

In this section, the theory presented in Sec. II is experimentally checked. For this purpose we work in the limit of low propagating velocity in a narrow channel (W = 17.5 mm). For different small positive and negative angles ($|\ \omega\ | < 1°$) and large B values ($0.06 < B < 0.1$) corresponding to a finger width $\lambda \approx 0.85$, we measure the remaining oil thicknesses $\delta_t^{2/3}$ and $\delta_b^{2/3}$. The first result is that gravity is very efficient for breaking the finger symmetry. Indeed in this channel, gravity forces are of the same order as surface tension forces for a tilt angle of 0.4°. Air fingers are then very accurate (but very slow) levels. Taking into account numerical values in Eqs. (17), (25), and (26) we can write Eqs. (27) and (28) as

$$\delta_b^{2/3} \approx 0.100 - 0.290(B - 0.763\sigma) \qquad (32)$$

and

$$\delta_t^{2/3} \approx 0.100 - 0.290(B + 0.763\sigma). \qquad (33)$$

Thus, a linear dependence of $(\delta_b^{2/3} - \delta_t^{2/3})$ with σ is predicted. This is well confirmed experimentally (Fig. 5) except that the experimental slope is 1.15 when theory predicts 0.44. We will come back to this numerical discrepancy. In Fig. 6 the evolution of $\delta_b^{2/3}$ vs $(B - 0.763\sigma)$ and $\delta_t^{2/3}$ vs $(B + 0.763\sigma)$ is plotted. By this choice of abscissa, the two data sets now collapse on the same linear curve. This is again in agreement with our theory and confirms its main result: for slightly tilted cells and large fingers, the selection law of the finger's width is unchanged as soon as the parameter B is replaced by $B \mp \sigma/A$. However, there is again a numerical discrepancy since experimentally the best linear fit gives $\delta_i^{2/3} \approx 0.22 - 0.75(B \mp 0.763\sigma)$ (for $i = t, b$) while Dombre and Hakim [20] as well as our theoretical predictions give Eqs. (32) and (33) in the limit of $\lambda \to 1$. This discrepancy is ascribed to the fact that the experiments correspond to $\lambda \approx 0.85$ where the theory is no longer

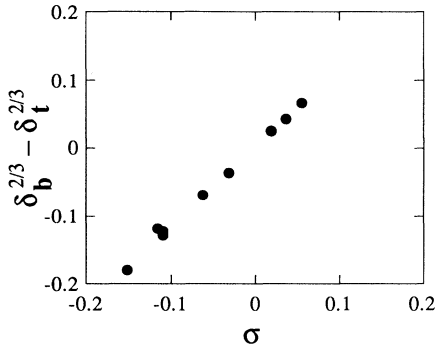

FIG. 5. Evolution of $(\delta_b^{2/3} - \delta_t^{2/3})$ vs gravity parameter σ. The best linear fit gives $(\delta_b^{2/3} - \delta_t^{2/3}) \approx 1.15\sigma$ $(0.066 \leq B \leq 0.083)$.

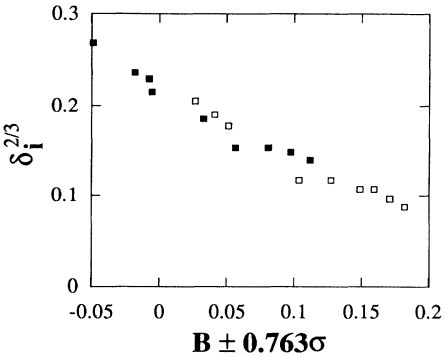

FIG. 6. Superposition of the two data sets: $\delta_b^{2/3}$ vs $(B - 0.763\sigma)$ (■)and $\delta_t^{2/3}$ vs $(B + 0.763\sigma)$ (□). B evolves between 0.066 and 0.083, σ between -0.15 and $+0.06$. The best linear fit gives $\delta_i^{2/3} \approx 0.22 - 0.75(B \mp 0.763\sigma)$ with $i = t, b$.

quantitatively correct. However, as shown by Tabeling, Zocchi, and Libchaber [4] three-dimensional effects of the wetting on the sidewalls become dominant in the limit of $\lambda \to 1$, and the selection law is replaced by $(1 - \lambda) \sim 1/B$. So we compared, in the same range of B values $(0.05 < B < 0.2)$, our experimental data with the experiments of Tabeling, Zocchi, and Libchaber [4] (best linear fit: $\delta_i^{2/3} \approx 0.22 - 0.69B$) and with numerical simulations by Ben Amarand simultaneously Yuhai Tu [25] (best linear fit: $\delta_i^{2/3} \approx 0.27 - 1.03B$). Our experimental data of Fig. 6 are in very good agreement with these two results. We then confirm experimentally that the gravity correction in the selection relation of Ref. [20] is equivalent to replace the term AB by the term $AB \mp \sigma$ in Eqs. (27) and (28). The disagreement with theoretical numerical factors is the very same disagreement observed for symmetrical ST fingers when $\lambda < 1$ between theory on the one hand and numerical simulations or experiments on the other hand.

IV. CONCLUSION

In this paper we presented theoretical and experimental results on the selection of stable Saffman-Taylor fingers propagating in tilted Hele-Shaw cells. At large velocity, even for very low tilt angle, we observed drastic changes: fingers are very narrow and propagate near the upper side of the cell. When their speed is increased these fingers broaden, in contrast to the usual case, and are less asymmetrical. We agree with the estimation of Brener, Levine, and Tu [18], suggesting large gravity effects for angles of the order of few degrees. The general evolution is in agreement with their theoretical predictions although we were not able to check precisely the scaling laws. At low velocity we revisited the selection theory in order to take gravity-induced asymmetry into account. We proved experimentally that the gravity effect was correctly predicted as it allows one to recover experimental and numerical results of symmetrical ST fingers.

Initially, Hele-Shaw cells have been introduced as a model for simulating flows in porous media and the major technological interest in viscous fingering is in understanding the instability of diphasic flows in real three-dimensional porous reservoirs where gravity is always important. Here we pointed out in this simple case the important asymmetry that gravity can induce when fluids are density contrasted. In all classical viscous fingering experiments using gas as the low viscosity fluid, it is only by careful adjustment of the levelness that, until now, experimentalists have removed the effect of gravity.

ACKNOWLEDGMENTS

We thank V. Hakim and M. Ben Amar for discussions. One of us (E.B.) acknowledges financial support from a grant of the DRET (France). The Laboratoire de Physique Statistique de L'Ecole Normale Supérieure is "associé au CNRS et aux Universités Paris VI et Paris VII."

* Permanent address: Institute for Solid State Physics, Academy of Sciences, 142432 Chernogolovka, Russia.

[1] Y. Couder, in *Chaos, Order and Patterns*, edited by R. Artuso, P. Cvitanovic, and G. Casati, NATO ASI Series B: Physics Vol. 280 (Plenum, New York, 1991) p. 203; D. Bensimon, L.P. Kadanoff, S. Liang, B.I. Shraiman, and C. Tang, Rev. Mod. Phys. **58**, 977 (1986).

[2] P. G. Saffman and G. I. Taylor, Proc. R. Soc. London, Ser. A **245**, 312 (1958).

[3] R. Combescot, T. Dombre, V. Hakim, Y. Pomeau, and A. Pumir, Phys. Rev. Lett. **56**, 2036 (1986); Phys. Rev. A **37**, 1270 (1988); D. C. Hong and J. Langer, Phys. Rev. Lett. **56**, 2032 (1986); B. Shraiman, *ibid.* **56**, 2028 (1986).

[4] P. Tabeling, G. Zocchi, and A. Libchaber, J. Fluid Mech. **177**, 67 (1987).

[5] Y. Couder, N. Gerard, and M. Rabaud, Phys. Rev. A **34**, 5175 (1986).
[6] H. Thomé, R. Combescot, and Y. Couder, Phys. Rev. A **41**, 5739 (1990).
[7] M. Ben Amar, Phys. Rev. A **43**, 5724 (1991); Yuhai Tu, Phys. Rev. A **44**, 1203 (1991).
[8] H. Thomé, M. Rabaud, V. Hakim, and Y. Couder, Phys. Fluids A **21**, 224 (1989).
[9] M. Rabaud and V. Hakim, in *Instabilities and Nonequilibrium Structures III*, edited by E. Tirapegui and W. Zeller (Kluwer Academic, Norwell, MA, 1991), p. 217.
[10] H. Cummins, L. Fourtune, and M. Rabaud, Phys. Rev. E. **47**, 1727 (1993).
[11] J.T. Gleeson, P.L. Finn, and P.E. Cladis, Phys. Rev. Lett. **66**, 236 (1991).
[12] G. I. Taylor and P. G. Saffman, Q. J. Mech. Appl. Math. **12**, 265 (1959).
[13] G. Zocchi, B.E. Shaw, A. Libchaber, and L.P. Kadanoff, Phys. Rev. A **36**, 1894 (1987).
[14] M. Rabaud, Y. Couder, and N. Gerard, Phys. Rev. A **37**, 935 (1988).
[15] D.C. Hong, Phys. Rev. A **39**, 2042 (1989).
[16] S. Tanveer, Phys. Fluids **30**, 1589 (1987).
[17] R. Combescot and T. Dombre, Phys. Rev. A **38**, 2573 (1988).
[18] E. Brener, H. Levine, and Y. Tu, Phys. Fluids A **3**, 529 (1991).
[19] To our knowledge the only case where the effect of gravity that has been previously studied is in horizontal thick cells by M. H. Jensen, A. Libchaber, P. Pelcé, and G. Zocchi, Phys. Rev. A **35**, 2221 (1987). They showed that at low velocity, the vertical asymmetry of the meniscus makes the two wetting films left on the glass plates unequal.
[20] T. Dombre and V. Hakim, Phys. Rev. A **36**, 2811 (1987).
[21] L. Landau and B. Levich, Acta Physicochim. URSS **17**, 42 (1942).
[22] J. D. Weeks and W. van Saarloos, Phys. Rev. A **39**, 2772 (1989).
[23] S. Tanveer, Proc. R. Soc. London, Ser. A **428**, 511 (1990).
[24] J. F. Nye, H.W. Lean, and A.N. Wright, Eur. J. Phys. **5**, 73 (1984).
[25] M. Ben Amar (private communication).